JOINT EUROPEAN TORUS JET

JET–P(93)26

J.T. Berndtson, J.A. Heikkinen, S.J. Karttunen,
T.J.H. Pättikangas, R.R.E. Salomaa

Analysis of Velocity Diffusion of Electrons with Vlasov-Poisson Simulations

Analysis of Velocity Diffusion of Electrons with Vlasov-Poisson Simulations

J.T. Berndtson[1], J.A. Heikkinen[1], S.J. Karttunen[2],
T.J.H. Pättikangas[2], R.R.E. Salomaa[1]

JET-Joint Undertaking, Culham Science Centre, OX14 3DB, Abingdon, UK

[1]Helsinki University of Technology, Nuclear Engineering Laboratory, Espoo, Finland.
[2]Technical Research Centre of Finland, Nuclear Engineering Laboratory, Espoo, Finland.

Preprint of a paper to be submitted for publication in
Plasma Physics and Controlled Fusion
April 1993

ABSTRACT

Wave-induced velocity diffusion is studied with a one-dimensional relativistic Vlasov-Poisson code. The diffusion coefficient is determined by following test electrons in the self-consistent electrostatic field formed by a narrow spectrum of electron plasma waves. The diffusion coefficient is found to be slightly larger than the quasilinear value at intermediate values of Chirikov's overlap parameter. The largest deviation is about 20 to 30%. At higher values of the overlap parameter, the diffusion is slower than quasilinear for a small number of field modes, but faster than quasilinear for a large number of the modes.

1. INTRODUCTION

In tokamak plasmas, the wave-induced current obtained in rf current drive is usually calculated from the Fokker-Planck equation by using the quasilinear diffusion coefficient (BONOLI and ENGLANDE, 1986; BERS and RAM, 1992). After the original work of VEDENOV et al. (1961) and DRUMMOND and PINES (1962), several generalisations of the quasilinear theory have been investigated. Some of these models predict diffusion coefficients that differ considerably from the quasilinear value at certain parameter regions.

DUPREE (1966) and WEINSTOCK (1969) developed resonance broadening theory, which gives a small correction to the quasilinear diffusion coefficient. The direct interaction approximation originally developed for Navier-Stokes turbulence was applied to Vlasov turbulence by ORSZAG and KRAICHNAN (1967). DUPREE ((1972) formulated the so-called clump theory, which in addition to the quasilinear diffusion also includes anomalous friction. The clump theory was developed to a self-consistent renormalized perturbation theory by BOUTROS-GHALI and DUPREE (1981). ADAM et al. and LAVAL and PESME (1983, 1984) introduced the turbulent trapping model, which takes into account the non-Gaussian statistics of the electrostatic field caused by the nonlinear mode coupling. The turbulent trapping model predicts an enhancement of the diffusion coefficient by a factor of 2.2 compared to the quasilinear value.

A simple method for examining the validity of the quasilinear theory is to follow an ensemble of test electrons in a prescribed field of electrostatic waves. The behaviour of the test electrons depends crucially on the value of the overlap parameter (CHIRIKOV, 1979). The electron trajectories become stochastic in the

momentum space, when the trapping regions of the Fourier modes E_k overlap significantly. This occurs when the overlap parameter

$$\epsilon_k(t) = \frac{|q_e E_k(t)/k|}{m_e(\Delta v_{ph})^2} = \left(\frac{v_{tr}}{2\Delta v_{ph}}\right)^2 \qquad (1)$$

becomes large. Here, the trapping width is denoted by $v_{tr} = 2|q_e E_k/m_e k|^{1/2}$ where k is the wave number of the mode, and q_e and m_e are the electron charge and mass, respectively. The spacing of the modes is $\Delta v_{ph} = |v - v_g(k)|\,\Delta k/k$, where v and v_g are the phase and the group velocity corresponding to the wave number k, respectively. Note that for $\epsilon_k = 1/16$ the trapping regions of the modes just start to overlap each other, i.e. $v_{tr} = \Delta v_{ph}/2$.

Several important results on the validity of the quasilinear approximation have previously been obtained by test particle calculations in prescribed electric fields. The quasilinear estimate has been shown to be valid (CHIRIKOV, 1979) in the limit of large overlap parameter (1). Deviations in the intermediate ϵ_k-region have been found by RECHESTER and WHITE (1980), by CARY et al. (1990), and by JENSEN and OBERMAN (1982).

CARY et al. (1990) investigated the diffusion caused by randomly phased modes of the electrostatic field. The found that the diffusion coefficient exceeds the quasilinear estimate at about $\epsilon_k = 0.3$, and reaches the maximum $D = 2.3D_{QL}$ near $\epsilon_k = 1$. For increasing ϵ_k, the diffusion coefficient approaches from above the quasilinear limit without obtaining smaller values than D_{QL}. In these simulations, convergence of the diffusion coefficient was obtained for overlap parameters $\epsilon_k = 0$ to 6 when the number of the modes was larger than 600.

CHIRIKOV (1979) and RECHESTER and WHITE (1980) studied the case of the exactly phased modes. They predicted an oscillatory behaviour of the diffusion coefficient as a function of the overlap parameter, but found the quasilinear limit at large values of ϵ_k.

The self-consistent electrostatic field was taken into account in the simulations by THEILHABER et al. (1987), who studied the weak beam-plasma instability. The simulation parameters were chosen in order to test the predictions of the turbulent trapping model. THEILHABER et al. (1987) found that the growth rate of the instability was by a factor of 1.2 to 1.6 larger than the quasilinear growth

rate. The diffusion coefficient was not directly determined in these simulations. However, one can see from momentum conservation arguments that the diffusion was enhanced by the same factor as the growth rate. In the simulations, the enhancement of the diffusion was therefore somewhat smaller than the factor 2.2 predicted by the turbulent trapping model.

In the present paper, the relativistic one-dimensional Vlasov and Poisson equations are solved for a system of waves which are adiabatically turned on. In contrast to earlier work (THEILHABER et al., 1987), we take into account the finite temperature of the bulk electrons, which yields realistic dispersion properties of the waves. We make a direct measurement of the diffusion coefficient from the simulation data, and compare the results with the quasilinear theory. For simplicity, the plasma is modelled as homogeneous and infinite by using periodic boundary conditions. The waves are taken to form a narrow spectrum with up to 33 externally excited modes which have phase velocities from $v_{ph} = 3.2v_e$ to $3.9v_e$. The diffusion coefficient is evaluated by solving the equations of motion for test electrons by using the self-consistent electric field obtained from the Vlasov-Poisson solution.

The present simulations deal with the electron plasma waves. In the high frequency limit, the lower hybrid waves can be considered as magnetized electrostatic electron plasma waves. In this limit, the dispersion relation of the lower hybrid waves is approximately $\omega^2 = \omega_p^2 k_\parallel^2 / k_\perp^2$, where $k_\parallel^2 << k_\perp^2$, and $k_\parallel^2$ and $k_\perp^2$ refer to the wave numbers parallel and perpendicular to the magnetic field, respectively. Our one-dimensional Vlasov-Poisson simulation is therefore analogous to solving the velocity distribution of the electrons in the direction parallel to the magnetic field for lower hybrid waves.

The paper is organised as follows: In Section 2, the model equations for the simulations are presented. A method for estimating the diffusion coefficient from the results of the simulations is described in Section 3. In Section 4, the diffusion coefficient is compared to the quasilinear theory. The time evolutions of the distribution function and of the electrostatic field are also investigated. The origin of the broadening of the electrostatic spectrum and of the diffusion regime are discussed. Finally, Section 5 contains a brief summary.

2. MODEL EQUATIONS

In test particle calculations, the stochastic motion of the electrons in the momentum space is determined by a prescribed electric field. Solution of both the Vlasov and Poisson equations makes it possible to investigate the evolution of the momentum distribution in the self-consistent electric field determined by the electron distribution. This approach takes into account the nonlinear Landau damping and the mode-coupling effects (LAVAL and PESME, 1983), which are caused by the nonlinear term in the Vlasov equation. Inclusion of these effects may affect the diffusion, when the amplitudes of the modes are large.

In a one-dimensional electron plasma, the relativistic Vlasov and Poisson equations are

$$\frac{\partial f}{\partial t} + \frac{p}{m_e \gamma}\frac{\partial f}{\partial z} + q_e E \frac{\partial f}{\partial p} = 0 \tag{2}$$

$$\frac{\partial E}{\partial z} = \frac{q_e n_e}{\varepsilon_0}\left[\int f dp - 1\right], \tag{3}$$

where n_e is the electron density. These one-dimensional equations provide a simple enough system for routine numerical studies.

To study the momentum diffusion of the electrons, consider the spectrum of waves

$$\begin{aligned} E(z,t) &= \sum_{k>0} E_k(t)\ \cos\left(kz - \omega_k t - \varphi_k\right) \\ &= \frac{1}{2}\sum_{k\neq 0} E_k(t)\ \exp\left[i(kz - \omega_k t - \varphi_k)\right], \end{aligned} \tag{4}$$

where the wave numbers are $k = 2\pi n/L$ in a box of length L, and φ_k is the initial phase. We assume that one frequency ω_k can be assigned to each mode. The Fourier components of the electric field are defined by

$$E_k(t) = \frac{2}{L}\int_{-L/2}^{L/2} E(z,t)\ \exp\left[-i(kz - \omega_k t - \varphi_k)\right] dz. \tag{5}$$

In equations (4) and (5), we have adopted the notation $E_{-k} = E_k$ and $\omega_{-k} = -\omega_k$ and $\varphi_{-k} = -\varphi_k$.

3. DIFFUSION IN MOMENTUM SPACE

3.1 Quasilinear diffusion

In the quasilinear theory, the space-averaged Vlasov equation is approximated by the diffusion equation (DRUMMOND and PINES, 1963); KAUFMAN, 1972)

$$\frac{\partial f_0}{\partial t} = \frac{\partial}{\partial p} D_{QL} \frac{\partial f_0}{\partial p}, \tag{6}$$

where the slowly-varying space-averaged distribution function is defined by $f_0(p,t) = L^{-1} \int_{-L/2}^{L/2} f(z,p,t)\ dz$.

According to the quasilinear theory, the diffusion coefficient of the electrons in the momentum space is

$$D_{QL}(p,t) = \frac{\pi}{2} q_e^2 \sum_{k>0} E_k^2(t) \delta(\omega_k - kv). \tag{7}$$

In the continuum limit, the sum on the right-hand side yields

$$D_{QL}(p,t) = \frac{\pi q_e^2}{2k\Delta v_{ph}} E_k^2(t), \tag{8}$$

where k is the root of the equation $v = \omega_k/k$. The resonant velocities are spaced by $\Delta k = 2\pi/L$.

3.2 Diffusion in Vlasov-Poisson simulations

The one-dimensional equations of motion for a single relativistic test electron in the field of the electrostatic waves are

$$\frac{dp}{dt} = v \tag{9}$$

$$\frac{dp}{dt} = q_e E(z, t), \tag{10}$$

where v and p are the velocity and the momentum of the electron in the z-direction.

The diffusion coefficient is obtained as the rate of change of the momentum variance

$$D(p,t) = \frac{1}{2}\frac{d}{dt}\left\{\left\langle\left[\Delta p(t)\right]^2\right\rangle - \left\langle\Delta p(t)\right\rangle^2\right\}, \qquad (11)$$

where $\Delta p(t) = p(0)$ is the momentum increment, and $\langle\ \rangle$ stands for an ensemble average. Hence, the diffusion coefficient can be determined by solving the momentum variance as a function of time for a group of test electrons which have the initial momentum p(0). The trajectories are solved by leapfrog scheme which is similar to the one presented by GHIZZO et al. (1993).

In Vlasov-Poisson simulations of the velocity diffusion, we assume periodic boundary conditions which correspond to infinite interaction region. The Vlasov and Poisson equations (2)-(3) are solved by the method introduced by CHENG and KNORR (1976) (see also GHIZZO et al., 1990). The advantage of this Eulerian method over the particle-in-cell simulations is that the code is almost noiseless.

At the beginning of the simulation, the electron distribution is a relativistic Maxwellian. The electrostatic waves are excited in the plasma by external fields which are of the form given in equation (4). The oscillation frequencies $\omega_k = \omega(k)$ of the external field components are estimated from the linear dispersion relation of the electron plasma wave. The driving fields are turned on adiabatically in the beginning of the simulation and turned off before $\omega_p t \simeq 100$. The diffusion coefficient is measured in the self-consistent field after $\omega_p t = 250$.

In a periodic box of finite length L, the wave numbers have to satisfy the relation $k = 2\pi n/L$, which together with the dispersion relation determines the spacing of the phase velocities of the modes. The simulation of a large number of modes having a narrow phase velocity spectrum requires a large box compared to the wavelengths of modes. This sets an upper limit to the number of the modes which can be simulated within reasonable CPU time. Typically, the evolution of up to 50 modes can be followed in the phase velocity region $0.7v_{p0} - 1.3v_{p0}$, where v_{p0} stands for the average

phase velocity of the spectrum. A more detailed description of the numerical methods used and of the code has been given by BERNDTSON and PÄTTIKANGAS (1992).

4. VLASOV-POISSON SIMULATIONS

In order to compare the diffusion coefficient (11) to the quasilinear estimate (8), we consider cases where $2N + 1 = 9$, 17 and 33 waves are excited in the plasma by external fields. The wave numbers of the external fields are in the range $k\lambda_D = 0.3$ to 0.4, and the corresponding phase velocities vary from $v_{ph} = 3.21v_e$ to $3.87v_e$. In this wave number range, all the $2N + 1$ modes which were compatible with the periodic boundary conditions were excited. The separation of the modes was therefore $\Delta k\lambda_D = 0.1/2N$. In the present simulations, the electron density was $n_e = 10^{20}$ m^{-3} and the temperature was $T_e = 1$keV.

4.1 Plateau formation

The time evolution of the Fourier components of the field is shown in Fig. 1, where nine external field components excite the waves. After the excitation at $\omega_{pt} > 100$, the Fourier components oscillate and decay gradually. After $\omega_{pt} \simeq 200$, the oscillations are damped and a quasi-steady state is approached.

We define the average of the Fourier amplitudes as

$$E = \left\{ (2N+1)^{-1} \sum_k E_k^2 \right\}^{1/2}, \qquad (12)$$

where $2N + 1$ is the number of the driving field components. In Fig. 2, the average Fourier amplitude of the nine components is shown. The time evolution of the average is much smoother than that of the individual Fourier components in Fig. 1. The steady state has not yet been reached at $\omega_{pt} = 300$.

The space-averaged electron distribution $f_0(p,t)$ is shown in Fig. 3 at various times. The trapping width in the momentum space is also shown for each Fourier component. Only nine waves were excited between $k\lambda_D = 0.3$ and 0.4 by the external field. The resulting spectrum, however, is

broader due to several new Fourier components outside the initial wave number region. This is most likely caused by the mode-coupling which will be discussed in Section 4.3.

The distribution function is considerably deformed already at $\omega_p t = 100$, and the plateau forms by $\omega_p t = 300$, the steady state is reached, and there are only minor variations in the Fourier components and in the distribution function.

4.2 Diffusion coefficient

We first study the momentum diffusion in the middle of the plateau region, between $p/m_e c = 0.1436$ and 0.1736 in Fig. 3, by using the method described in Section 3.2. Fig. 4 illustrates the time dependence of the momentum variance $\langle \Delta p^2 \rangle$ for seven ensembles with different p(0), when nine Fourier components of the field have been excited. For each initial momentum, the momentum variance is calculated for an ensemble of 128 test electrons having different z(0). The saturation levels of the momentum variances vary between $\langle \Delta p^2 \rangle / m_e^2 c^2 = 5 \times 10^{-4}$ and 8×10^{-4}.

In Fig. 5, the diffusion coefficient (11) in the momentum region between $p/m_e c = 0.1436$ and 0.1736 is determined from the rate of change of the average of the momentum variances of Fig. 4. The diffusion coefficient is estimated from the steepest slope of the variance, i.e. before the saturation caused by the finite width of the spectrum (ISHIHARA et al., 1992).

Fig. 6 shows the diffusion coefficient obtained from the simulations and normalized to the quasilinear value (8) as a function of the overlap parameter (1). The overlap parameter was calculated from the average of the Fourier amplitudes that was presented in equation (12). The diffusion coefficient was calculated for the average seven ensembles as was discussed above.

In Fig. 6, the diffusion coefficients are shown for 9, 17 and 33 externally excited modes. All the three cases seem to exhibit the same qualitative behaviour. At small values of the overlap parameter, the diffusion coefficient stays above the quasilinear value. The largest deviation is about

20 to 30%. At higher values of ϵ_K, the diffusion is slower than quasilinear for 9 and 17 modes, but faster than quasilinear for 33 modes.

In the derivation of the quasilinear theory, it is assumed that the autocorrelation time of the wave is short compared to the evolution times of the electric field and the averaged distribution function. The autocorrelation time is defined by $\tau_{ac} = \delta k^{-1} \left| v - v_g \right|^{-1}$, where δk is the width of the spectrum. In our simulations, we had $\delta k \lambda_D \simeq 0.1$ and hence $\omega_p \tau_{ac} \simeq 3.8$. Note that the momentum variance grows as $\left\langle \Delta p^2 \right\rangle \sim t^2$ at $\omega_p t - 250 << \omega_p \tau_{ac}$ in the beginning of the measurement of the diffusion coefficient (cf. Figs 4 and 5).

The evolution time of the electric field was large in our simulation because we measured the diffusion coefficient close to a steady state. For 33 modes, the evolution time of the electric field at $\omega_p t = 250$ was $\omega_p t_E > 1000$ at all values of the overlap parameter. For 9 modes, we had $\omega_p t_E \simeq 50$ for intermediate overlap parameters ($\epsilon_k \simeq 1$), and $\omega_p t_E \simeq 450$ at large values of the overlap parameter ($\epsilon_k \sim 6$). For 9 modes, the plateau was not yet fully developed by $\omega_p t = 250$ for intermediate overlap parameters, and therefore the evolution time of the field was so short. In all cases, however, the assumption $\tau_{ac} << t_E$ was well satisfied.

The evolution time of the space-averaged distribution function is $t_f = m^2 / \left(k^2 D_{QL} \tau_{ac}^2 \right)$. At intermediate values of the overlap parameter ($\epsilon_k \simeq 1$), we find $\omega_p t_f \simeq 1200$ and 79000 for 9 and 33 modes, respectively. When the overlap parameter is large ($\epsilon_k \simeq 6$), we find $\omega_p t_f \simeq 34$ and 2200 for 9 and 33 modes, respectively. Therefore, the assumption $\tau_{ac} << t_f$ is valid in the simulation of 9 modes even in the large amplitude region where the diffusion is slower than quasilinear. In this parameter region, the bounce time for the simulation of 9 modes at $\epsilon_k \simeq 6$ is $\omega_p t_f \simeq 78$, which is large compared to the autocorrelation time.

ADAM et al. (1979) and LAVAL and PESME (1983, 1984) have derived an additional condition for the validity of the quasilinear theory. According to their model for 'turbulent trapping', the field amplitudes must be so small that $t_E << \tau_{RB}$, where $\tau_{RB} = (k^2 D_{QL} / m^2)^{-1/3}$ is the resonance broadening time. Otherwise, the mode-coupling effects will give rise to non-Gaussian

statistics of the field which will enhance the diffusion. The refined threshold for the enhanced diffusion is $t_E \geq t\tau_{RB}$ (THEILHABER et al., 1987). According to the turbulent trapping model, the diffusion coefficient is $D = 2.2D_{QL}$ in this parameter region (LAVAL and PESME, 1984).

The limit of the large evolution time of the field in the turbulent trapping model is interesting for the current drive applications, where the formation of the plateau decreases the damping rate of the waves. In the parameter region $\epsilon_k \simeq 1$, where we find enhanced diffusion in our simulations, we have $\omega_p\tau_{RB} \simeq 26$ and 105 for 9 and 33 modes, respectively. Since we have $\omega_p t_E > 1000$ for 33 modes, the condition for the enhanced diffusion $t_E \geq 5\tau_{RB}$ is valid in our simulations. On the other hand, we also found enhanced diffusion for 9 modes in the region $\epsilon_k \simeq 1$, where $\omega_p t_E \simeq 50$ and the condition $t_E \geq 5\tau_{RB}$ is not valid. In all cases, the enhancement of the diffusion that we find is also considerably smaller than the prediction of the turbulent trapping model.

The diffusion coefficients obtained in simulations with five modes, which are not shown in Fig. 6, behave irregularly already at fairly small values of the overlap parameter. Similar irregular features are found for nine excited modes, but at larger values of the overlap parameter and the width of the spectrum are kept constant in equation (1), the amplitudes of the Fourier components become larger if the number of the modes decreases. The spacing of the modes Δv_{ph} also becomes larger when the number of the modes decreases. The discreteness of the spectrum is described by the discretization time $\tau_d = 2\pi/k\Delta v_{ph}$, i.e., the time it takes for an electron to resolve the separate Doppler frequencies of the modes (CARY et al., 1992). In our simulations, we had $\omega_p\tau_d \simeq 190$ and 760 for 9 and 33 modes, respectively.

4.3 Mode-coupling effects

All the generalisations of the quasilinear theory that were discussed in Section 1 involve the treatment of the nonlinear term in the Vlasov equation (2), i.e. the mode-coupling term. The second order nonlinear terms lead to modes with wave numbers $k = 0$ or $\pm 2k_1$, where k_1 is a typical wave number in the original narrow spectrum. Since the natural frequency of these second harmonic waves is very different from $\omega = 0$ or

$2\omega_1$, the second order nonlinear coupling is weak (DRUMMOND AND PINES, 1962). The enhanced diffusion of the turbulent trapping model is caused by the third and higher odd order nonlinear terms (LAVAL and PESME, 1983). These terms can drive modes that have wave numbers close to the original narrow spectrum. For instance, if we have the modes $k_1 \simeq$) $k_2 \simeq k_3$ in the wave spectrum, the phase matching condition yields $k = k_1 + k_2 - k_3 \simeq k_1$.

As the first numerical experiment on the mode coupling, we investigated the broadening of the spectrum in Fig. 3, where the external fields had the wave numbers from $k\lambda_\Delta = 0.3$ to 0.4. We performed a simulation whereby only every second of the modes allowed by the periodic boundary conditions were excited by the external fields. In other words, the modes from $k\lambda_D = 0.3$ to 0.4 with step $2\Delta k\lambda_D = 0.0125$ were excited externally in a simulation where the step size of the allowed modes was $\Delta k\lambda_D = 0.00625$. In such a simulation, we found that the spectrum became wider so that new modes with wave numbers $k\lambda_D = 0.3 - 2n\Delta k\lambda_D$ and $k\lambda_D = 0.4 + 2n\Delta k\lambda_D$ were generated (cf. Fig. 3). No modes were found with wave numbers of the form $k\lambda_D = \left(n + \frac{1}{2}\right)2\Delta k\lambda_D$. The reason for this is probably that the phase matching conditions discussed above yield only such wave numbers that are multiples of $2\Delta k$.

The simulation shown in Fig. 7 is similar to the one described above except that we have added an extra Fourier component at $k\lambda_D = 0.35625$ to the spectrum of the external fields. Therefore, in this simulation the phase matching conditions of the form $k = k_1 + k_2 - k_3$ can also yield such wave numbers that are of the form $k\lambda_D = \left(n + \frac{1}{2}\right)2\Delta k\lambda_D$. In Fig. 7 such modes can be seen to grow between the externally driven Fourier modes in the interval $k\lambda_D = 0.3$ to 0.4. After the external fields have been turned off at $\omega_p t \simeq 100$, the spectrum evolves towards equilibrium which is achieved at $\omega_p t \simeq 300$.

In the spectra of Fig. 7, one can see a signal around $k\lambda_D \simeq 0.7$, which is the second harmonic of the waves of the original spectrum. At $\omega_p t = 80$, there is a gap in the spectrum between $k\lambda_D = 0.4$ and 0.6 which is filled due to generation of new modes by $\omega_p t = 300$. Modes at very low amplitude are also excited in the long-wavelength region near $k\lambda_D \simeq 0$. These signals are caused by the second order nonlinear term in the Vlasov equation.

So far, we have assumed that the electrostatic field can be written as a sum of Fourier modes (4), where all the modes obey the linear dispersion relation. In order to investigate this assumption, we have calculated the space and time Fourier transformation of the electric field

$$E_{k,\omega} = \frac{1}{TL}\int_0^T dt \int_{-L/2}^{L/2} dz E(z,t)\exp[-i(kz-\omega t)]. \qquad (13)$$

Fig. 8 shows the frequency spectra $E_{kj,\omega}$ for the first harmonic ($k_1\lambda_D = 0.35$) and the second harmonic ($k_2\lambda_D = 0.7$) in the simulation discussed above. The natural frequencies obtained from the linear dispersion relation would be for these modes $\omega_{k_1} = 1.22\omega_p$ and $\omega_{k_2} = 1.67\omega_p$, respectively. The second harmonic mode shown in Fig. 8 oscillates, however, with the frequency $\omega_2 \simeq 2.35\omega_p$, which is approximately the second harmonic frequency of the fundamental mode, i.e. $\omega_2 \simeq 2\omega_{k_1}$. A small-amplitude signal can also be seen at the natural oscillation frequency of the second harmonic at $\omega_{k_2} = 1.67\omega_p$.

In Fig. 3 the trapping regions of the modes are located at the phase velocities of the modes obtained from the linear dispersion relation, i.e. $v_{ph}(k) = \omega_k/k$. The discussion above reveals that such an interpretation of the wave number spectrum is to some extent incomplete. For instance, the phase velocity of the second harmonic mode should be approximately $v_{ph}(k_2) \simeq 2\omega_{k_1} = v_{ph}(k_1)$. This modifies the diffusion coefficient slightly near the lower boundary of the plateau. Note, however, that the amplitudes of the modes at large wave numbers are very small.

The second harmonic plasma wave at $k_2\lambda_D = 2k_1\lambda_D = 0.7$ and $\omega_2 = 2\omega_{k_1} = 2.44\omega_p$ is not a normal mode but a forced oscillation driven by the primary plasma wave. Therefore, we have $\mathrm{Re}\{\epsilon(\omega_2,k_2)\} \neq 0$ and $\mathrm{Re}\{\epsilon(\omega_1,k_1)\} = 0$, where $\epsilon(\omega,k)$ is the dielectric response function. We can find an order of magnitude estimate for the second harmonic mode with the aid of a simple mode-coupling model. The slowly-varying complex amplitude of the electron plasma wave can be estimated from

$$\frac{\partial E_2}{\partial t} - \frac{i\epsilon_2 E_2}{\partial\epsilon_2/\partial\omega_2} = -\frac{q_e k_1 E_1^2}{2m_e\omega_1^2\partial\epsilon_2/\partial\omega_2}, \qquad (14)$$

where $\epsilon_2 = \epsilon(\omega_2, k_2)$. In the case of a normal mode, the real part of the dielectric function would vanish so that the only contribution would be a small imaginary part. The second term on the left-hand side of equation (14) would then reduce to ΓE_2, where Γ is the damping decrement.

Since the second harmonic plasma wave is not an eigenmode, the second term on the left-hand side of equation (14) is large, and we can neglect the time derivative. At $\omega_p t = 300$, we have in the simulation the field $|E_1| \simeq 3.8 \times 10^5$ V / m, and $\omega_p = 5.64 \times 10^{11} s^{-1}$, and $\epsilon_2 = 0.76 + i0.02$. Hence, we obtain from equation (14) for the amplitude ratio $|E_2/E_1| \simeq 1.4 \times 10^{-3}$.

The situation is more complicated in the simulation than in the model equation (14). For instance, the mode $k_2\lambda_D = 0.7$ is driven by all the pairs of modes which satisfy the condition $k_i\lambda_D + k_j\lambda_D = 0.7$. Therefore, we should, in fact, have the terms corresponding all these pairs of modes on the right-hand side of equation (14). In Fig. 7 we have at $k\lambda_D = 0.35$ about ten modes within the full width to half maximum value at $\omega_p t = 300$. Therefore, we have in this range five pairs of modes that satisfy the phase matching condition. If we as an order of magnitude estimate multiply the amplitude ratio by this factor of five, we find $|E_2/E_1| \simeq 0.7 \times 10^{-2}$. This is by a factor of two smaller than the simulation result $|E_2/E_1| \simeq 1.3 \times 10^{-2}$ in Fig. 7 at $\omega_p t = 300$.

5. SUMMARY AND DISCUSSION

We have investigated the wave-induced velocity diffusion caused by a narrow spectrum of waves. The diffusion coefficient has been measured in the plateau region of the distribution in conditions where a steady state current is formed. The Vlasov simulations, where the electrostatic field is calculated self-consistently, make it possible to test models which predict deviations from the quasilinear theory. One of the most interesting of the recent theories is the turbulent trapping model, because it predicts enhanced diffusion in the limit where the evolution time of the field t_E is large compared to the resonance broadening time τ_{RB}. The enhancement of the diffusion is due to the mode-coupling effects which give rise to non-Gaussian statistics of the field.

In our Vlasov simulations, we had up to 33 externally excited modes with wave numbers from $k\lambda_D = 0.3$ to 0.4. Approximately 20 overlapping modes outside this

wave number region were generated during the simulation so that the total number of the overlapping modes was about 50. In the simulations (see Fig. 6) we observed diffusion that is faster than quasilinear by 20 to 30% at intermediate values of the overlap parameter ($\epsilon_k \simeq 1$). The assumption $t_E >> \tau_{RB}$ of the turbulent trapping model for the enhanced diffusion was valid in our simulations for 33 excited modes. We also observed enhanced diffusion at $\epsilon_k \simeq 1$ in the simulation for 9 excited m odes where $t_E \simeq 2\tau_{RB}$. The enhancement is, however, in all cases smaller than the prediction $D = 2.2D_{QL}$ of the turbulent trapping model.

It is interesting to note that the diffusion coefficients shown in Fig. 6 resemble qualitatively those obtained by CARY et al. (1990, 1992). They found an enhancement of the diffusion coefficient by a factor of 2.3 at $\epsilon_k \simeq 1$ in simulations with a randomly phased prescribed field. The enhancement that we find is smaller, but it occurs at the same value of the overlap parameter. CARY et al. (1992) have suggested that the mode-coupling effects cause an effective k-space discretization of the turbulence which enhances the diffusion. Therefore, the enhancement could also be seen in simulations with prescribed fields which have a discrete k-spectrum.

In the simulations with 33 externally excited modes, the diffusion co-efficient also stays slightly above the quasilinear value even in the region of large overlap parameters (see Fig. 6). In the simulation with 9 and 17 modes, we found diffusion that was slower than quasilinear when the overlap parameter was large ($\epsilon_k \simeq 6$). This was most likely caused by trapping of the electrons close to the resonances of the large-amplitude modes.

In the Vlasov simulations, we found evidence of mode-coupling effects. When the original wave number spectrum was between $k_1\lambda_D = 0.3$ and 0.4, the nonlinear coupling broadened the spectrum towards smaller and larger wave numbers. It was demonstrated that the second harmonic wave at $k_2\lambda_D 2k_1\lambda_D \simeq 0.7$ has the same phase velocity as the original wave, i.e. $v_{ph}(k_2) = 2\omega_{k_1}/2k_1$.

The Vlasov code has important limitations. The one-dimensional model does not behave correctly when we approach the steady state. In fact, the diffusion equation (6) has no steady state solution with $E_k \neq 0$ in two- or three-dimensions (BERNSTEIN and ENGELMANN, 1966). In the Vlasov model, we also have assumed fixed ions. This excludes, for instance, the wave-wave interactions with

the ion modes, which affects the results at large amplitudes. Investigation of these effects is left for further work.

ACKNOWLEDGEMENTS

The authors would like to thank Prof. P. BERTRAND and Dr. A. BERGMANN for useful discussions on solving the Vlasov-Poisson equations. The valuable discussions with Dr. D. PESME on the quasilinear theory are gratefully acknowledged. J.A.H. would like to thank Prof. D.F. Düchs and Dr. L.-G. Eriksson for their encouragement and interest. This research was partly supported by the Academy of Finland and the Finnish Ministry of Trade and Industry. This research was done under the JET contract No. JT1/13805.

REFERENCES

ADAM, J.C., LAVAL, G. and PESME, D. (1979) Phys. Rev. Lett. **43**, 1671.

BERNDTSON, J.T. and PÄTTIKANGAS, T.J.H. (1992) Report TKK-F-B137, Helsinki University of Technology, Espoo, 77 pp.

BERNSTEIN, I.B. and ENGELMANN, F. (1966) Phys. Fluids **9**, 937.

BERS, A. and RAM, A.K. (1991) in Proc. IAEA Technical Committee Meeting on Fast Wave Current Drive in Reactor Scale Tokamaks, Arles, France (Edited by D. Moreau, A. Bécoulet and Y. Peysson), p. 3.

BONOLI, P.T. and ENGLANDER, R.C. (1986) Phys. Fluids **29**, 2937.

BOUTROS-GHALI, T. and DUPREE, T.H. (1981) Phys. Fluids **24**, 1839.

CARY, J.R., ESCANDE, D.F. and VERGA, A.D. (1990) Phys. Rev. Lett. **65**, 3132.

CARY, J.R., DOXAS, I., ESCANDE, D.F. and VERGA, A.D. (1992) Phys. Fluids B **4**, 2062.

CHENG, C.Z. and KNORR, G. (1976) J. Comput. Phys. **22**, 330.

CHIRIKOV, B.V. (1970) Phys. Rep. **52**, 263.

DRUMMOND, W.E. and PINES, D. (1962) Nucl. Fusion Suppl. Part 3, 1049.

DUPREE, T.H. (1966) Phys. Fluids **9**, 1773.

DUPREE, T.H. (1972) Phys. Fluids **15**. 334.

GHIZZO, A., BERTRAND, P., SHOUCRI, M.M., JOHNSTON, T.W., FI-JALKOW, E. and FEIX, M.R. (1990) J. Comput. Phys. **90**, 431.

GHIZZO, A., BERTRAND, P., SHOUCRI, M., JOHNSTON, T. and LEBAS, J. (1933) Trajectories of Trapped Particles in the field of Plasma Wave Excited by a Stimulated Raman Scattering, to be published.

ISHIHARA, O., XIA, H and HIROSE, A. (1992) Phys. Fluids B **4**, 349.

JENSEN, R.V. and OBERMAN, C.R. (1982) Physica **4D**, 183.

KAUFMAN, A.N. (1972) J. Plasma Phys. **8**, 1.

LAVAL, G. and PESME, D. (1983) Phys. Fluids **26**, 52.

LAVAL, G. and PESME, D. (1984) Phys. Rev. Lett. **53**, 270.

ORSZAG, S.A. and KRAICHNAN, R.H. (1967) Phys. Fluids **10**, 1720.

RECHESTER, A.B. and WHITE, R.B. (1980) Phys. Rev. Lett. **44**, 1583.

THEILHABER, K., LAVAL, G and PESME, D. (1987) Phys. Fluids **30**, 3129.

VEDENHOV, A.A., VELIKHOV, E.P. and SAGDEEV, R.Z. (1961) Nucl. Fusion **1**, 82.

WEINSTOCK, J. (1969) Phys. Fluids **12**, 1045.

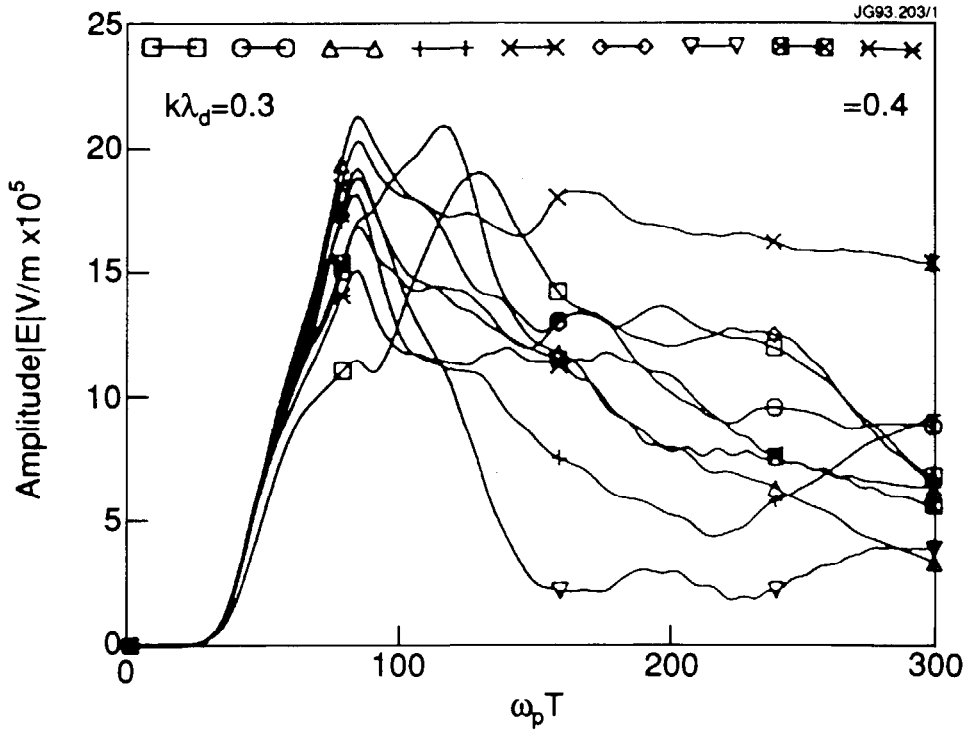

Fig. 1 Time dependence of the nine Fourier components $E_k(t)$ of the wave, when the wave numbers of the excited modes are between $d\lambda_D = 0.3$ and 0.4 ($n_e = 10^{20}m^{-3}$, $T_e = 1keV$).

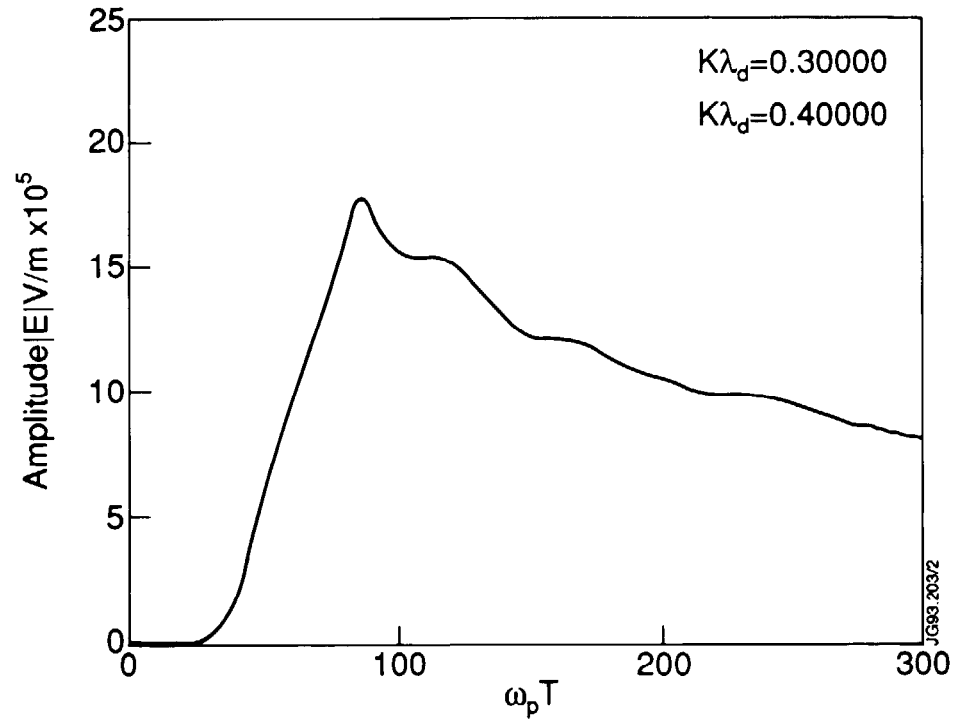

Fig. 2 The average amplitude (12) of the nine Fourier components shown in Fig. 1.

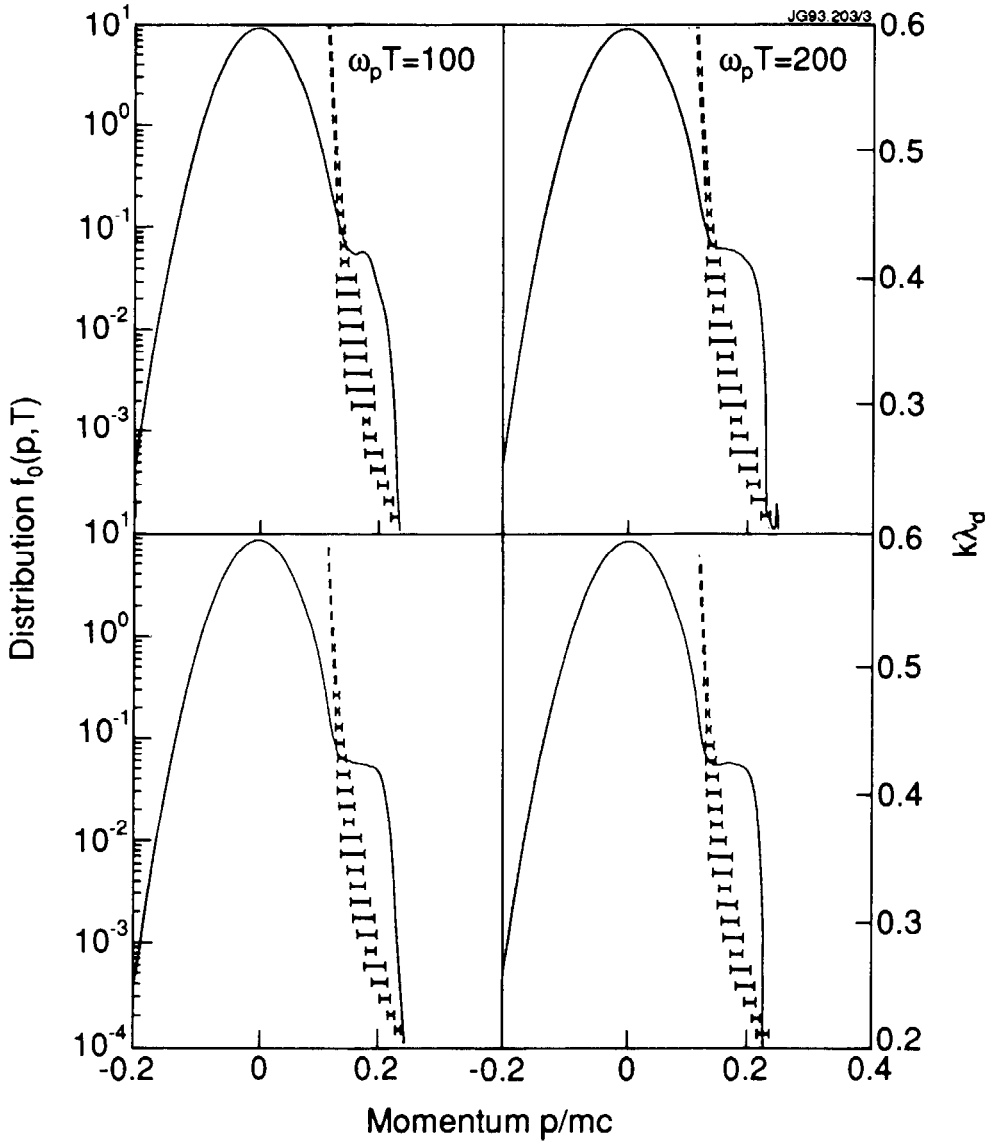

Fig. 3 The space-averaged momentum distributions $f_0(p,t)$ at $\omega_p t$ = 100, 200, 250 and 300, when nine modes are excited between $k\lambda_D$ = 0.3 and 0.4. The lines indicate the trapping widths of the Fourier components (see the right-hand scale).

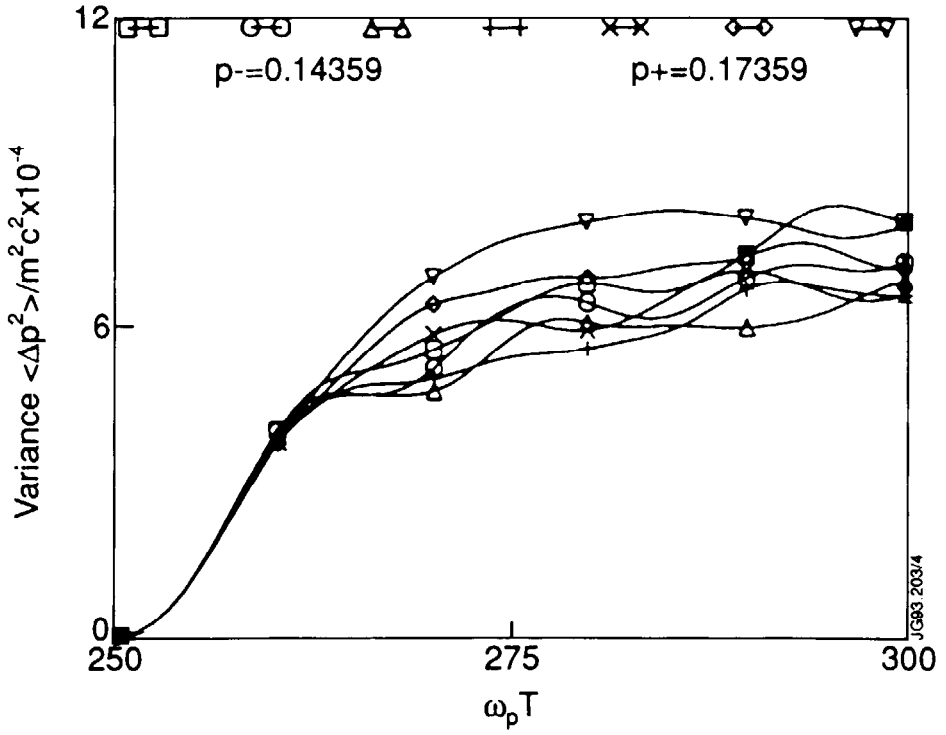

Fig. 4 The time behaviour of the momentum variance $\langle \Delta p^2 \rangle$ for seven ensembles, each consisting of 128 spatially distributed electrons. The initial momenta of the ensembles are between $p/m_e c = 0.1436$ and 0.1736.

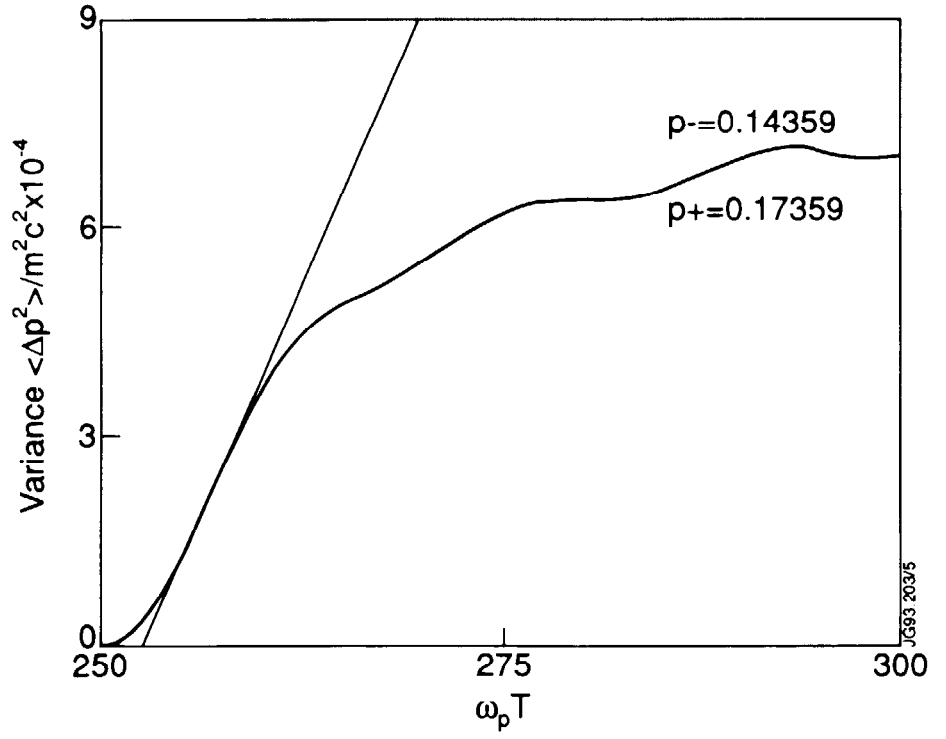

Fig. 5 The average of the momentum variances between $p/m_e c = 0.1436$ and 0.1736 versus time for the nine excited modes of Fig. 4 with $\epsilon_K = 6.9$. The diffusion coefficient in the momentum space (11) is evaluated from the steepest slope which is indicated by the straight line.

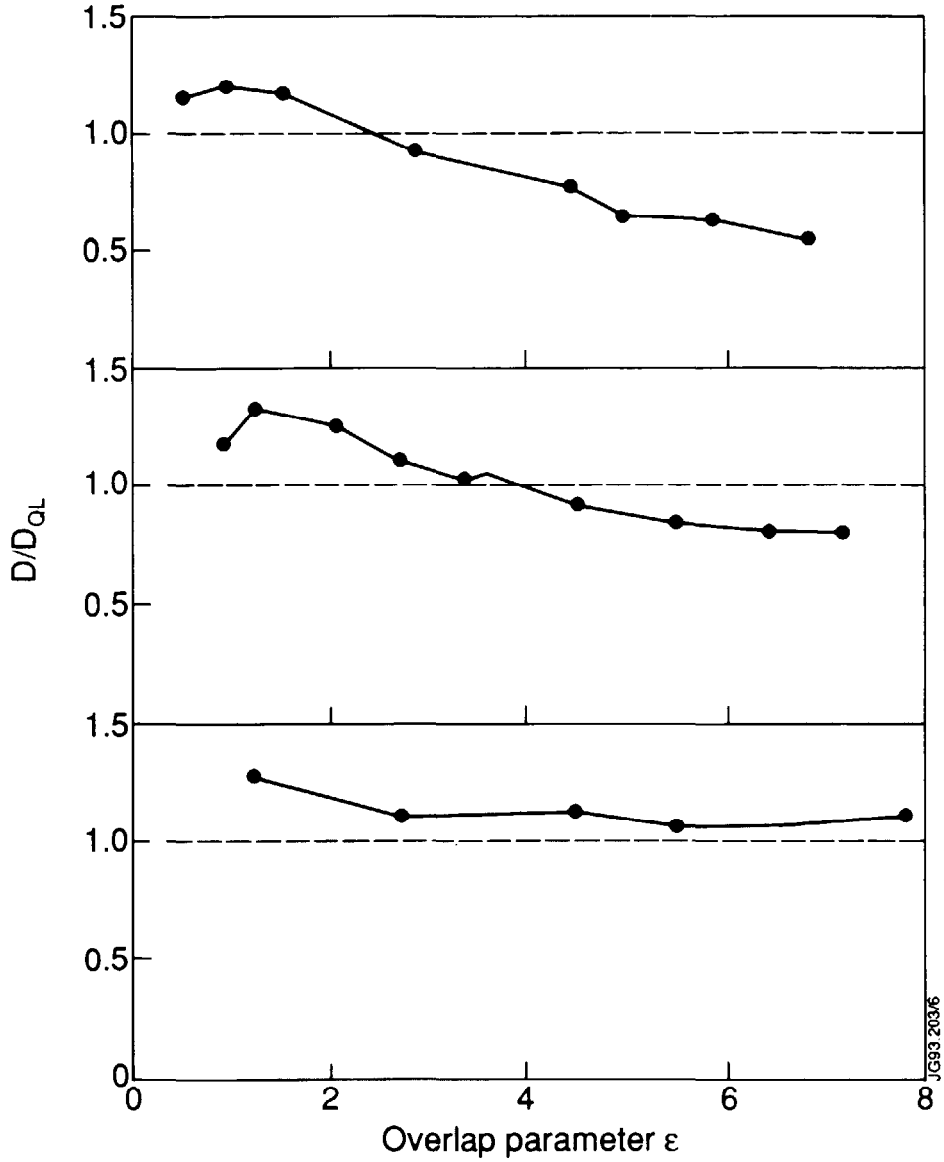

Fig. 6 The diffusion coefficients obtained from the simulations normalised to the quasilinear value (8), D/D_{QL}, versus the overlap parameter ϵ_K of equation (1). Results are shown from the simulations where 9 (top), 17 (middle) and 33 modes (bottom) were externally excited.

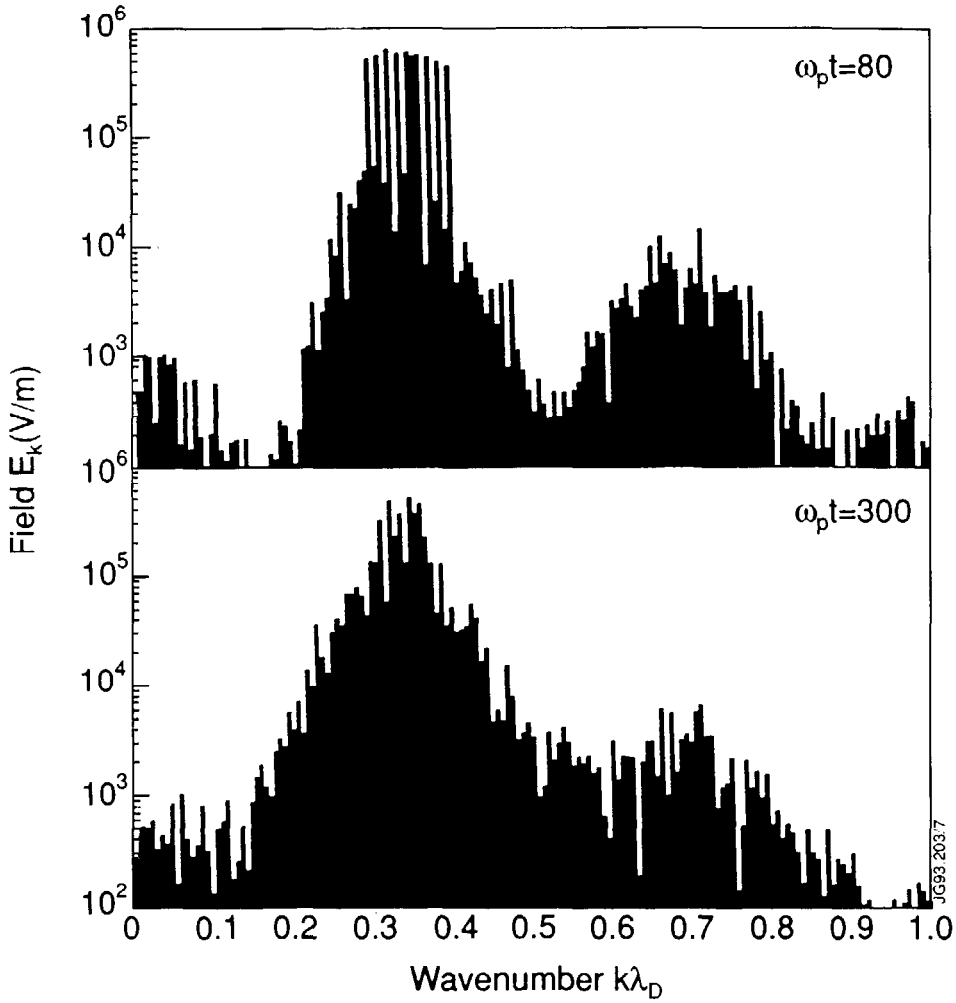

Fig. 7 The wave number spectrum of the electrostatic field at $\omega_p t = 80$ and $\omega_p t = 300$. The field is excited by ten external modes which are turned off at $\omega_p t \simeq$) 100. The wave numbers of the modes are between $k\lambda_D = 0.3$ and 0.4. The extra mode is at $k\lambda_D = 0.335625$. At $\omega_p t = 300$, the overlap parameter is $\epsilon_\kappa \simeq 8.7$.

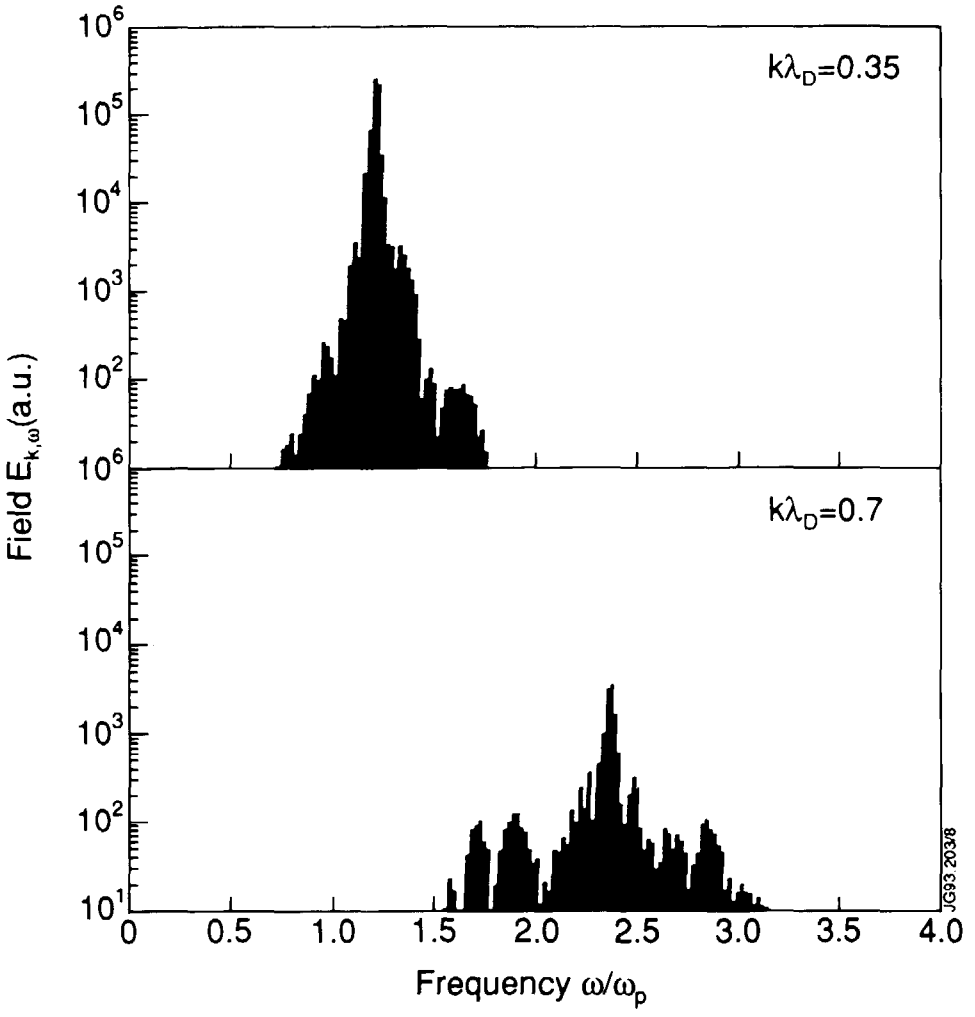

Fig. 8 The frequency spectra of the electrostatic wave for the wave number $k\lambda_D = 0.35$ and for the second harmonic mode $k\lambda_D = 0.7$. The Fourier transform in time has been calculated for the time interval $100 < \omega_p t < 400$.